Dalton Transactions

Accepted Manuscript

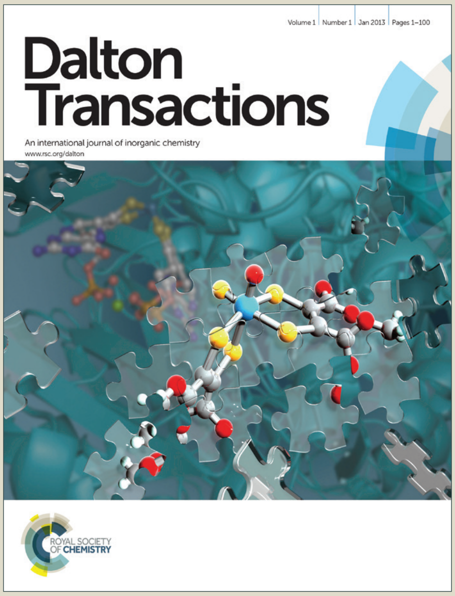

ROYAL SOCIETY OF CHEMISTRY

www.rsc.org/dalton

Journal Name RSCPublishing

ARTICLE

Cite this: DOI: 10.1039/x0xx00000x

Highly Emissive Copper(I) Complexes Bearing Diimine and Bis(diphenylphosphinomethyl)-2,2-dimethyl-1,3-dioxolane

Received 00th January 2012,
Accepted 00th January 2012

DOI: 10.1039/x0xx00000x

www.rsc.org/

Michihiro Nishikawa,[a] Shota Sawamura,[a] Aya Haraguchi,[a] Jun Morikubo,[a] Koichiro Takao[b] and Taro Tsubomura*[a]

A highly emissive copper(I) complex bearing (4*R*, 5*R*)-(-)-4,5-bis(diphenylphosphinomethyl)-2,2-dimethyl-1,3-dioxolane (diop) and 2,9-dimethyl-4,7-diphenyl-1,10-phenanthroline (dmpp), [Cu(dmpp)(diop)]PF_6 (**1**·PF_6), was newly synthesized. The quantum yield of the luminescence of **1**·PF_6 in degassed dichloromethane is 0.38, which is one of the highest values among all copper(I) complexes bearing two bidentate ligands, diimine and diphosphine, under the same condition. The long lifetime (26 μs) and high intensity of the emission come from the small non-radiative decay rate of the excited states. TD-DFT study indicates that the charge transfer transition from both copper and diphosphine to diimine orbitals plays an important role for the photophysical properties. Photophysics of [Cu(dmp)(diop)]PF_6 (**2**·PF_6, dmp = 2,9-dimethyl-1,10-phenanthroline) was also studied in order to reveal the effects of the introduction of the phenyl group at 4- and 7-positions of phenanthroline.

Introduction

Charge transfer (CT) excited state of metal complexes is one of the key features for photocatalysts and light-emitting devices due to their unique photochemical and photophysical properties.[1-6] Copper(I) complexes bearing two bidentate ligands are one of the promising candidates for these photofunctional materials.[5-36]

Up to now, bis(2-diphenylphosphinophenyl)ether (DPEphos) has been often used for the development of the photofunctional copper(I) complexes bearing diimine (NN) and diphosphine (PP) ligands due to their long lifetime and high quantum efficiency of the luminescence.[13-20] Diimine ligands, such as 2,9-dimethyl-1,10-phenanthroline (dmp) derivatives, are useful for the enhancement of the luminescence properties, because the methyl groups, which are close to the copper centre, effectively inhibit the structural rearrangement in the photoexcited states. Additionally, photophysics of the copper(I) complexes bearing 2,9-dimethyl-4,7-diphenyl-1,10-phenanthroline (dmpp) and DPEphos has been reported;[28] the substitution of the phenyl groups at 4- and 7- positions of the phenanthroline (Ph_{NN}) moiety has been found to increase the quantum yield and the lifetime of the luminescence.

Diop ((4*R*, 5*R*)-(-)-4,5-bis(diphenylphosphinomethyl)-2,2-dimethyl-1,3-dioxolane) had been widely used in the catalyst for asymmetric catalysis.[33] A few copper(I) complexes bearing diop, such as dinuclear copper(I) complex bridged by chloride anion, have been reported.[34] However, the number of reports about heteroleptic metal complexes bearing diimine and diop as well as their photophysical properties is limited.[35]

Scheme 1. Synthesis of [Cu(dmpp)(diop)]PF_6 (**1**·PF_6) and [Cu(dmp)(diop)]PF_6 (**2**·PF_6).

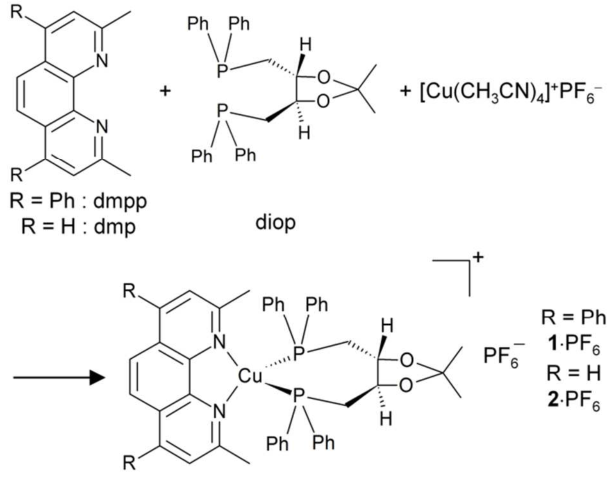

We have reported the photophysics of several emissive copper(I) complexes bearing dmp and diphosphine, such as dppe (1,2-bis(diphenylphosphino)ethane),[29] dppp (1,3-bis(diphenylphosphino)propane),[29] dppb (1,4-bis(diphenylphosphino)butane),[29] and BINAP (2,2′-bis(diphenylphosphino)-1,1′-binaphthyl).[30] We describe herein a highly emissive copper(I) complex bearing diop and dmpp, [Cu(dmpp)(diop)]PF_6 (**1**·PF_6) (Scheme 1). We also compare the photophysics of **1**·PF_6 with [Cu(dmp)(diop)]PF_6 (**2**·PF_6),[35] in order to discuss the effects of the introduction of Ph_{NN} on the photophysics of the complexes. Furthermore, comparison of $\mathbf{2}^+$ with previously reported $[Cu(dmp)(PP)]^+$ complexes[13,14,29] enables us to elucidate the ligand effects of diop moiety which drastically enhances the luminescence.

Experimental

Materials and Methods

(4*R*, 5*R*)-(-)-4,5-Bis(diphenylphosphinomethyl)-2,2-dimethyl-1,3-dioxolane (diop) was purchased from Strem Chemicals Inc.. 4,7-Diphenyl-2,9-dimethyl-1,10-phenanthroline (bathocuproine, dmpp) was purchased from Tokyo Chemical Industry CO., LTD. Tetrakis(acetonitrile)copper(I) hexafluorophosphate ($[Cu(MeCN)_4]PF_6$)[37a], $[Cu(dmpp)_2]PF_6$,[37b] and $[Cu(dmp)_2]PF_6$[37b] were synthesized according to the method described in the literature. ^{1}H-NMR, ^{13}C-NMR, and ^{31}P-NMR spectra in acetone-d_6 were recorded on a JEOL Delta-500 spectrometer using tetramethylsilane (δ = 0.00 ppm, ^{1}H) and solvent residual signals (δ = 29.84 ppm, ^{13}C) as internal standards,[38] and 85% phosphoric acid (δ = 0.00 ppm, ^{31}P) as an external standard. Absorption and emission spectra were obtained in a solvent degassed by at least five freeze-pump-thaw cycles using a quartz cell fitted with a Teflon vacuum stop cock. Absorption spectra were measured on a Shimadzu UV-3100 spectrometer. Emission spectra and emission lifetimes were collected on a laboratory-made apparatus. For the steady state emission spectra, a degassed sample solution was excited by a monochromated Xe lamp (a 75 W lamp connected to an Oriel Cornerstone 130 monochromator) and the emission was collected through a quartz fiber and fed into a spectrometer equipped with a cooled CCD sensor (Ocean Optics model QE65000). Emission quantum yields were obtained using $[Ru(bpy)_3]Cl_2$ as a standard (Φ = 0.094 in acetonitrile).[39] For the measurement of emission decay, the sample was excited by a N_2 laser (Usho, KEN-1520), and the emission was focused on a 20 cm monochromator (Jovin Yvon H-20). The emission light was detected by a photomultiplier tube, Hamamatsu R928, and the signal was digitized by an oscilloscope (Tektronix TDS5034).

Synthesis

$[Cu(dmpp)(diop)]PF_6$ ($1{\cdot}PF_6$). Under an argon atmosphere, $[Cu(MeCN)_4]PF_6$ (35 mg, 0.094 mmol) was added to diop (47 mg, 0.094 mmol) in a 5 mL tetrahydrofuran solvent. Then, dmpp (36 mg, 0.094 mmol) was added. The reaction mixture was stirred for 90 min. at room temperature. Diethyl ether was added to the solution to precipitate the product as a yellow solid, which was filtered, washed with diethyl ether, and dried in vacuo: yield, 53 mg (0.050 mmol, 53%). **^{1}H NMR** (500 MHz, acetone-d_6) δ 8.01 (s, 2H, phen), 7.66 (m, 12H), 7.52 (m,4H), 7.44 (t, 2H, J = 8 Hz), 7.37 (t, 2H, J = 8 Hz), 7.28 (t, 2H, J = 8 Hz), 7.22 (m, 4H), 7.13 (m, 4H), 4.67 (m, 2H), 3.52 (m, 2H), 3.19 (m, 2H), 2.36 (s, 6H), 1.53 (s, 6H). **^{13}C NMR** (126 MHz, acetone-d_6) δ 159.9, 151.3, 144.8, 137.6, 134.6, 134.4, 132.7 (t, J = 7 Hz), 131.9 (t, J = 7 Hz), 131.2, 130.7, 130.5, 130.2, 130.0 (t, J = 5 Hz), 129.9, 129.5 (t, J = 5 Hz), 126.8, 126.6, 124.8, 109.5, 81.0 (t, J = 10 Hz), 32.0 (t, J = 10 Hz), 28.1, 27.2. **^{31}P{^{1}H} NMR** (202 MHz, acetone-d_6) −21.0 (s, br, phosphine), −143.6 (septet, PF_6^-). Anal. Found: C, 64.12; H, 4.67; N, 2.71%. Calcd. for $1{\cdot}PF_6$, $C_{57}H_{52}N_2O_2F_6P_3Cu$: C, 64.13; H, 4.91; N, 2.62.

$[Cu(dmp)(diop)]PF_6$ ($2{\cdot}PF_6$). Synthesis of $2{\cdot}ClO_4$ has been mentioned in the literature.[35] $2{\cdot}PF_6$ was synthesized according to a similar procedure to that of $1{\cdot}PF_6$ with a modification of the solvent from tetrahydrofuran to CH_2Cl_2. **^{1}H NMR** (500 MHz, acetone-d_6) δ 8.70 (d, 2H, J = 8 Hz, phen), 8.24 (s, 2H, phen), 7.73 (d, 2H, J = 8 Hz, phen), 7.42 (m, 6H, Ph), 7.31 (t, J = 8 Hz, 4H, Ph), 7.24 (t, J = 8 Hz, 2H, Ph), 7.15 (m, 4H, Ph), 7.06 (t, J = 8 Hz, 4H, Ph), 4.66 (m, 2H), 3.51 (m, 2H), 3.15 (m, 2H), 2.25 (s, 6H), 1.53 (s, 6H). **^{13}C NMR** (126 MHz, acetone-d_6) δ 160.4, 144.0, 139.3, 134.5, 134.4, 132.5 (t, J = 7 Hz), 131.8 (t, J = 7 Hz), 131.1, 130.7, 129.9 (t, J = 4 Hz), 129.5 (t, J = 4 Hz), 129.1, 127.3, 126.4, 109.5, 81.0 (t, J = 10 Hz), 32.0 (t, J = 10 Hz), 27.8, 27.2. **^{31}P{^{1}H} NMR** (202 MHz, acetone-d_6) −21.7 (s, br, phosphine), −143.6 (septet, PF_6^-). Anal. Found: C, 58.88; H, 4.62; N, 3.47%. Calcd. for $2{\cdot}PF_6$, $C_{45}H_{44}N_2O_2F_6P_3Cu$: C, 59.05; H, 4.85; N, 3.06.

Crystallography

X-ray crystallographic measurements of $1{\cdot}PF_6{\cdot}2THF$ and $2{\cdot}PF_6{\cdot}CH_2Cl_2$ were made on a Rigaku Saturn 70 CCD area detector with graphite-monochromated MoKα radiation. Images were collected and the data were processed by using *CrystalClear*.[40] The structures were solved by direct methods *SIR-92*[41] and refined by full matrix least squares procedures (*SHELXL-97*).[42] All calculations were performed by using the *Wingx* crystallographic software package.[43] Crystallographic data have been deposited with Cambridge Crystallographic Data Centre: Deposition number CCDC-1020906 for $1{\cdot}PF_6{\cdot}2THF$ and CCDC-1020905 for $2{\cdot}PF_6{\cdot}CH_2Cl_2$. Copies of the data can be obtained free of charge via http://www.ccdc.cam.ac.uk/conts/retrieving.html. Single crystals suitable for analysis were obtained by slow diffusion of hexane in tetrahydrofuran or dichloromethane solution of $1{\cdot}PF_6$ or $2{\cdot}PF_6$, respectively. Crystal data of $1{\cdot}PF_6{\cdot}2THF$: $C_{67}H_{52}N_2O_2F_6P_3Cu$, M_r=1187.56, yellow crystal, orthorhombic, space group $P2_12_12_1$, a = 11.3979(7) Å, b = 21.1386(11) Å, c = 25.6198(16) Å, $\alpha = \beta = \gamma$ = 90°, V = 6172.7(6) Å^3, Z = 4, T = 123 K, D_c = 1.278 g cm^{-3}, μ = 0.494 mm^{-1}, R = 0.0737 for 12781 reflections with $I > 2\sigma(I)$, R_w = 0. 2188 GOF = 1.06, Flack parameter 0.001(14); Crystal data of $2{\cdot}PF_6{\cdot}CH_2Cl_2$: $C_{46}H_{46}N_2O_2F_6P_3Cl_2Cu$, M_r= 1000.2, yellow crystal, triclinic, space group $P1$, a = 9.927(9) Å, b = 11.073(10) Å, c = 11.197(11) Å, α = 90.23(3)°, β = 90.84(3)°, γ = 112.89(3)°, V = 1133.6(18) Å^3, Z = 1, T = 123 K, D_c = 1.465 g cm^{-3}, μ = 0.771 mm^{-1}, R = 0.0558 for 5952 reflections with $I > 2\sigma(I)$, R_w = 0.138 GOF = 1.032 Flack parameter -0.014(16).

DFT calculation

Calculation was performed using Gaussian 03W software[44] with the B3LYP[45-47] method using the atomic coordinates determined by X-ray as the initial coordinates in the optimization. TDDFT was used to calculate singlet and triplet excited state energies. Basis sets were as follows: copper 6-311G with Wachters's 4p functions,[48] phosphorus, oxygen, and nitrogen 6-31G*+, carbon 6-31G*, and hydrogen 6-31G. Population analysis was carried out by *AOMIX* software.[49] The pictures of the orbitals have been depicted with *MOLKEL* software.[50]

Results and Discussion

$1{\cdot}PF_6$, was newly synthesized by a reaction of diop, dmpp, and tetrakis(acetonitrile)copper(I) hexafluorophosphate ($[Cu(MeCN)_4]PF_6$) in tetrahydrofuran at room temperature. The compound was characterized by ^{1}H NMR, elemental analysis, and single-crystal X-ray structural analysis.

Crystal structures of 1^+ and 2^+ are shown in Fig. 1. The structures of heteroleptic mononuclear copper(I) complexes

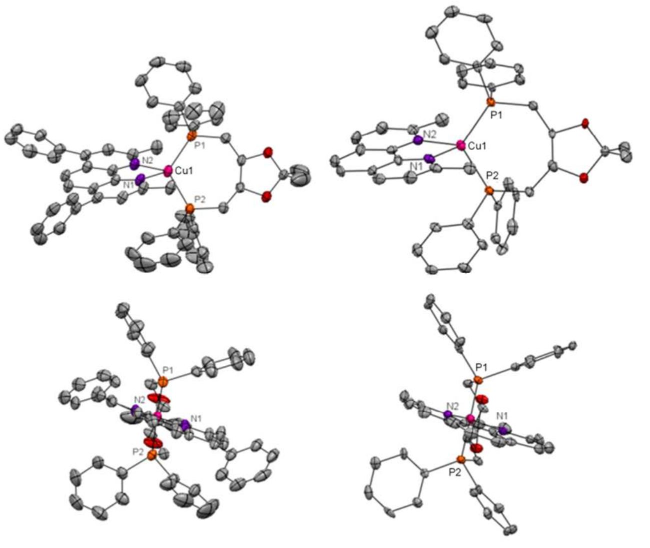

1$^+$
[Cu(dmpp)(diop)]$^+$

2$^+$
[Cu(dmp)(diop)]$^+$

Fig. 1. The crystal structures of the complex cations of **1**$^+$ (left) and **2**$^+$ (right). Hydrogens, counter ions, and solvent molecules are omitted for clarity. Important bond length (Å) and angles (°) for **1**$^+$: Cu1–N1, 2.060(3); Cu1–N2, 2.080(4); Cu1–P1, 2.2279(12); Cu1–P2, 2.2449(11); N1–Cu1–N2, 80.97(13); P1–Cu1–P2, 116.25(4). For **2**$^+$: Cu1–N1, 2.075(5); Cu1–N2, 2.084(5); Cu1–P1, 2.228(2); Cu1–P2, 2.258(2); N1–Cu1–N2, 81.3(2); P1–Cu1–P2, 114.71(8).

bearing two bidentate ligands, diimine and diphosphine, with tetrahedral coordination geometry were confirmed in both **1**$^+$ and **2**$^+$. The bond lengths, angles, and dihedral angles of these complexes were comparable to those in a family of copper(I) complexes bearing diimine and diphosphines (Table S1). The P-Cu-P angles of **1**$^+$ and **2**$^+$ are 116.25(4)° and 114.71(4)°, respectively. The P-Cu-P angle of **2**$^+$ is larger than that of [Cu(dmp)(dppp)]$^+$ (105.42(3)° and 105.31(3)°), and is similar to that of [Cu(dmp)(DPEPhos)]$^+$ (116.44(4)°). The dihedral angle between N-Cu-N and P-Cu-P planes of **1**$^+$ (81.0°) is smaller than those of **2**$^+$ (84.7°), indicating that the introduction of Ph$_{NN}$ increases the distortion of four-coordinated copper(I) complexes from regular tetrahedral geometry. The dihedral angle is also smaller than that observed in [Cu(dmp)(dppe)]$^+$ (89.5°, 87.2°), and [Cu(dmp)(dppp)]$^+$ (86.2°, 83.8°). The dihedral angles between Ph$_{NN}$ and phenanthroline planes in **1**$^+$ are 52° and 49°, suggesting that the π-conjugation of the phenanthroline moiety is not apparently extended to the Ph$_{NN}$ groups.

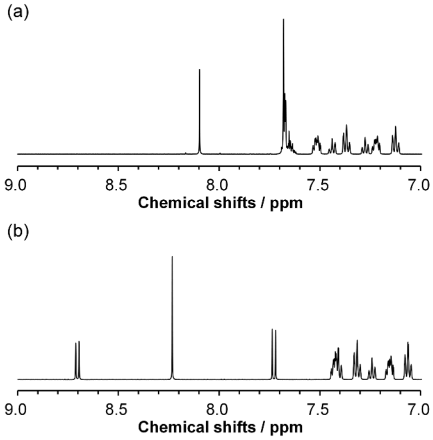

Fig. 2. Partial ^{1}H NMR spectra of **1**·PF$_6$ (a) and **2**·PF$_6$ (b) in acetone-d_6 at room temperature.

^{1}H NMR spectra of both **1**$^+$ and **2**$^+$ in acetone-d_6 at room temperature suggests that the heteroleptic structures are kept in the solution state. Other species, such as [Cu(dmpp)$_2$]PF$_6$ (δ = 8.16 and 8.00 ppm in acetone-d_6) and [Cu(dmp)$_2$]PF$_6$ (δ = 8.76, 8.23, and 7.98 ppm in acetone-d_6), are negligible, since only one set of aromatic signals of phenanthroline moieties is observed in the ^{1}H NMR spectra of both **1**$^+$ (δ = 8.01 and 7.66 ppm) and **2**$^+$ (δ = 8.70, 8.24 and 7.73 ppm) (Fig. 2 and Supplementary Information Fig. S1-S6). The chemical shifts in the ligand moieties, such as alkyl chain of diop, in ^{1}H NMR spectra of both **1**$^+$ and **2**$^+$ are shifted downfield from those of the free ligand, diop, because of the decrease of the electron density caused by coordination (Table S2). The downfield shifts of chemical shifts are also observed in ^{31}P NMR spectra (–21.0 ppm for **1**$^+$, –21.7 ppm for **2**$^+$, and –22.4 ppm for diop). Moreover, the ratios of signal integrations of diop and diimine moieties are also consistent with the heteroleptic compounds. ^{1}H NMR signals did not change after several days in air-saturated acetone-d_6 at room temperature (Fig. S7). Additionally, ^{1}H NMR spectrum of **1**$^+$ in dimethylsulfoxide-d_6/D$_2$O (v/v 10:1) after heating at 353 K for 2 hours under air is essentially the same as that before heating, suggesting that **1**$^+$ has sufficient stability even in the presence of water and highly coordinative solvent (Fig. S8). Heating **1**$^+$ in dimethylsulfoxide-

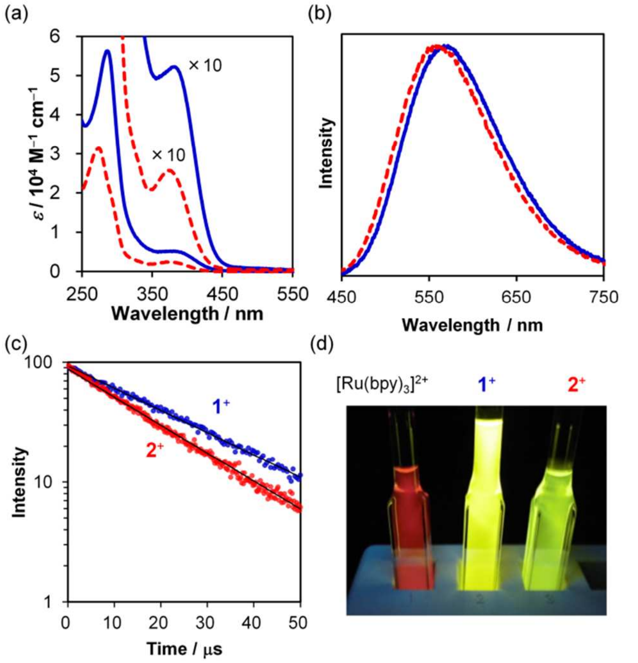

Fig. 3. (a) Absorption spectra of **1**·PF$_6$ (blue, solid line) and **2**·PF$_6$ (red, dashed line) in dichloromethane at room temperature. (b) Emission spectra of (blue, solid line) and **2**·PF$_6$ (red, dashed line) in degassed dichloromethane at room temperature. Excitation wavelength is 370 nm. (c) Emission decay curve of **1**·PF$_6$ (blue) and **2**·PF$_6$ (red) in degassed dichloromethane at room temperature observed at 580 nm. (d) Photograph of the emission of (left) [Ru(bpy)$_3$]Cl$_2$ in degassed acetonitrile, (middle) **1**·PF$_6$ in degassed dichloromethane, and (right) **2**·PF$_6$ in degassed dichloromethane at room temperature excited by UV light.

Table 1. Photophysical properties of the copper(I) complexes. All data were obtained in degassed dichloromethane at room temperature.

	$\lambda_{\mathrm{abs.max}}$ / nm	$\lambda_{\mathrm{em.max}}{}^{a}$ / nm	τ / µs	Φ^{a}	$k_r{}^{b}$ /10^4 s^{-1}	$k_{nr}{}^{c}$ /10^4 s^{-1}
1·PF$_6$	286, 382	570	26.1	0.38	1.4	2.4
2·PF$_6$	274, 374	560	17.7	0.30	1.7	4.0

a) λ_{ex} = 345 nm. b) $k_r = \Phi / \tau$. c) $k_{nr} = (1-\Phi) / \tau$.

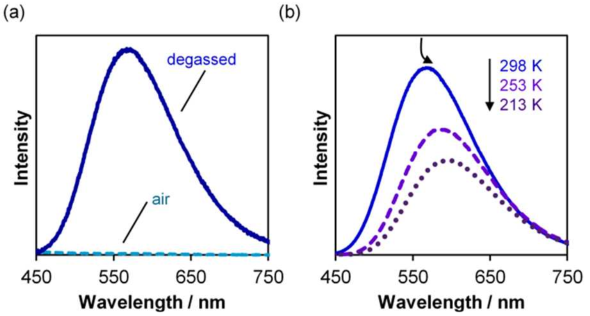

Fig. 4. (a) Emission spectra of **1**·PF$_6$ in degassed dichloromethane (blue, solid line) and in air-saturated dichloromethane (light blue, dashed line) at room temperature. (b) Emission spectra of **1**·PF$_6$ in degassed dichloromethane at 298 K (blue, solid line), at 253 K (purple, dashed line), and at 213 K (dark purple, dotted line).

d_6 at 393 K for 2 hours under air also induces nearly no change in ^{1}H NMR signals (Fig. S9). The high stability could be attributed to the instability of bis(diop) complex compared to **1**$^+$ in the disproportion equilibrium of two equivalent of [Cu(NN)(PP)]$^+$ into [Cu(NN)$_2$]$^+$ and [Cu(PP)$_2$]$^+$; the equilibrium is often observed in a family of copper(I) complexes bearing diimine and diphosphine.

Photophysical data of **1**$^+$ and **2**$^+$ in CH$_2$Cl$_2$ at room temperature are shown in Fig. 3a–3d and Table 1. Absorption spectra of both **1**$^+$ and **2**$^+$ show intense absorption around 280 nm due to π-π* transition (Fig. 3a). The values of λ_{abs} and molar extinction coefficient at the wavelength, ε, of **1**$^+$ are 286 nm and 5.6×10^4 M^{-1}cm^{-1}, and those of **2**$^+$ are 274 nm and 3.1×10^4 M^{-1}cm^{-1} (Table 1). Low-energy absorption is also observed in both complexes (λ_{abs} = 382 nm and $\varepsilon = 5.2\times10^3$ M^{-1}cm^{-1} for **1**$^+$; λ_{abs} = 374 nm and $\varepsilon = 2.6\times10^3$ M^{-1}cm^{-1} for **2**$^+$). The absorption is characteristic of the CT transition (Cu + P → diimine) in a family of [Cu(NN)(PP)]$^+$.[9-11] The wavelength of the CT absorption band of **2**$^+$ is blue-shifted from those of [Cu(dmp)(dppe)]PF$_6$ (λ_{abs} = 405 nm),[29] [Cu(dmp)(dppp)]PF$_6$ (λ_{abs} = 391 nm),[29] and [Cu(dmp)(DPEPhos)]BF$_4$ (λ_{abs} = 383 nm)[14] in dichloromethane at room temperature. The correlation of the blue-shift and the P-Cu-P angle has been reported;[29] blue-shift of the absorption peak of the diop complexes might be due to the large P-Cu-P angles. An absorption shoulder originated by [Cu(NN)$_2$]$^+$, which has been often observed near 470 nm in a family of [Cu(dmp)(PP)]$^+$,[12,29] was negligible in both **1**$^+$ and **2**$^+$. The wavelengths of both π-π* and CT transitions of **1**$^+$ are red-shifted from those of **2**$^+$, because the introduction of Ph$_{NN}$ groups considerably affects frontier orbitals of the complexes. The enhancement of ε of **1**$^+$ compared to **2**$^+$ is also caused by the introduction of Ph$_{NN}$; the effects have been reported in the literatures related to bis(diimine)copper(I) complexes.[32]

The emission spectra of both **1**$^+$ and **2**$^+$ show broad luminescence bands due to the CT excited state, which is characteristic of a family of [Cu(NN)(PP)]$^+$ complexes (Fig. 3b). The wavelength at the emission maximum, λ_{em}, of **1**$^+$ and **2**$^+$ are λ_{em} = 570 nm and λ_{em} = 560 nm, respectively. Furthermore, the difference in the Stokes shift of **1**$^+$ (8700 cm^{-1}) and **2**$^+$ (8800 cm^{-1}) is very small (100 cm^{-1}). The result can be explained by the small difference in the structural rearrangement in the photoexcited states between **1**$^+$ and **2**$^+$. The maximum wavelength of the CT luminescence of **2**$^+$ is blue-shifted from those of [Cu(dmp)(dppe)]PF$_6$ (λ_{em} = 594 nm),[29] [Cu(dmp)(dppp)]PF$_6$ (λ_{abs} = 600 nm),[29] and [Cu(dmp)(DPEphos)]BF$_4$ (λ_{em} = 565 nm)[14] in dichloromethane at room temperature. In the solid state, strong emissions are observed for complexes **1**$^+$ and **2**$^+$. The wavelength at the emission maximum of **1**$^+$ in the solid state under air at room temperature is red-shifted from that of **2**$^+$ (Fig. S10). The difference in the emission maxima could be caused by the difference between the two crystal structures. **1**$^+$ has more distorted tetrahedral geometry than **2**$^+$ as mentioned above.

The quantum yield, Φ, of the CT luminescence of **1**$^+$ in degassed dichloromethane at room temperature is 0.38, which is one of the highest values for copper(I) complexes bearing diphosphine and diimine ligands. The value is slightly larger than that of **2**$^+$ (0.30) under the same condition, suggesting that the introduction of Ph$_{NN}$ contributes to the enhancement of the quantum yield. The value of **2**$^+$ is higher than those of [Cu(dmp)(dppe)]$^+$ (0.01)[29] and [Cu(dmp)(dppp)]$^+$ (0.04)[29], and comparable with that of [Cu(dmp)(DPEphos)]$^+$ (0.15),[14,52] indicating that the diop ligand is effective to enhance the luminescence.

The emission decay curves of **1**$^+$ and **2**$^+$ in degassed dichloromethane are best fit to a single-exponential function (Fig. 3c). The lifetimes of the emission, τ, of **1**$^+$ and **2**$^+$ in degassed dichloromethane are 26.1 µs and 17.7 µs, respectively, suggesting that the Ph$_{NN}$ substitution extends the lifetime of the luminescence. The long lifetime of both **1**$^+$ and **2**$^+$ compared to normal organic fluorescence attributes to the fact that the emission of [Cu(NN)(PP)]$^+$ are often derived from delayed fluorescence.[9-12] The value of **2**$^+$ is much longer than those of [Cu(dmp)(dppe)]$^+$ (1.3 µs)[29] and [Cu(dmp)(dppp)]$^+$ (5.4 µs),[29] and is comparable with that of [Cu(dmp)(DPEPhos)]$^+$ (14.3 µs).[14]

The apparent radiative rate constant, k_r,[51] of **1**$^+$ (1.4×10^4 s^{-1}) is similar to that of **2**$^+$ (1.7×10^4 s^{-1}); k_r includes two radiative processes from both the excited singlet and triplet

Table 2. Population analysis of the DFT calculations based on the singlet optimized structures.

	K-S orbital	Energy / eV	Cu$^{a)}$	PP$^{b)}$	NN$^{c)}$	Ph$_{NN}$ $^{c)}$
1$^+$	LUMO+1	-4.05	0	1	90	9
	LUMO	-4.2	3	1	89	7
	HOMO	-7.71	54	34	9	3
	HOMO-1	-8.14	78	4	17	1
	HOMO-2	-8.35	76	16	8	0
	HOMO-3	-8.49	6	7	56	31
	HOMO-4	-8.73	11	1	26	62
2$^+$	LUMO+1	-4.22	0	1	99	–
	LUMO	-4.41	3	1	96	–
	HOMO	-7.9	57	37	6	–
	HOMO-1	-8.36	80	5	15	–
	HOMO-2	-8.5	76	17	8	–
	HOMO-3	-8.96	2	91	7	–
	HOMO-4	-8.98	2	27	70	–

a)-c) Components for copper$^{a)}$, diphosphine$^{b)}$, diimine except phenyl group$^{c)}$ and phenyl group in diimine$^{d)}$ moieties / %.

Table 3. TDDFT results. Calculated transition wavelength, oscillator strength (*f*), components of the transitions.

	Singlets calculated using singlet-optimized structures				Triplets calculated using singlet-optimized structures			
	λ / nm	f	Components	Coefficients	λ / nm	f	Components	Coefficients
1$^+$	427	0.1199	HOMO-1 → LUMO	-0.109	476	0.0000	HOMO-21 → LUMO	-0.116
			HOMO → LUMO	0.677			HOMO-13 → LUMO+1	0.107
	403	0.0499	HOMO → LUMO+1	0.691			HOMO-11 → LUMO+1	-0.121
	334	0.0170	HOMO-3 → LUMO	0.163			HOMO-4 → LUMO	0.205
			HOMO-4 → LUMO+1	0.648			HOMO-3 → LUMO+1	-0.400
	321	0.1727	HOMO-14 → LUMO	-0.126			HOMO → LUMO	0.301
			HOMO-4 → LUMO	-0.322			HOMO → LUMO+1	0.453
			HOMO-3 → LUMO+1	0.577				
2$^+$	432	0.0628	HOMO → LUMO	0.684	470	0.0000	HOMO-3 → LUMO	-0.112
	405	0.0146	HOMO → LUMO+1	0.694			HOMO → LUMO	0.694

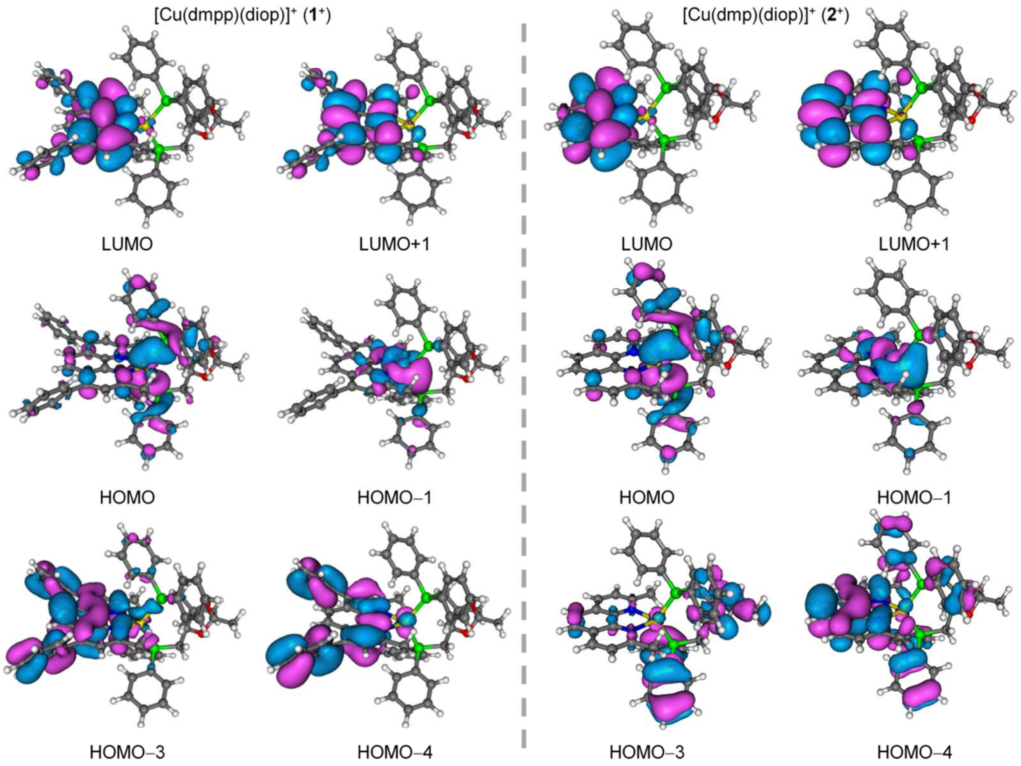

Fig. 5. Kohn-Sham orbitals of **1**$^+$ and **2**$^+$. Orbitals calculated based on the optimized structure in the S_0 (singlet ground) states (contour value 0.02).

states. The k_r of **2**$^+$ is larger than that of [Cu(dmp)(dppp)]$^+$ (0.7×10^4 s^{-1})[29], and comparable to that of [Cu(dmp)(DPEphos)]$^+$ (1.0×10^4 s^{-1})[52]. The non-radiative rate constants, k_{nr},[51] of **1**$^+$ and **2**$^+$ are 2.4×10^4 s^{-1} and 4.0×10^4 s^{-1}, respectively. The decrease in k_{nr} by introduction of Ph_{NN} could be explained by the inhibition of the solvent coordination in the excited state. The value of k_{nr} of **2**$^+$ is reduced from that of [Cu(dmp)(dppp)]$^+$ (1.8×10^5 s^{-1})[29] and from [Cu(dmp)(DPEphos)]$^+$ (6.0×10^4 s^{-1})[52]. The decrease in k_{nr} could be explained by the energy-gap law and the steric effects of rigid diop ligand in the excited states: the inhibition of the structural rearrangement and the inhibition of the solvent quenching. These two factors are often used to explain the photophysics of copper(I) complexes bearing diimine.[9-11]

The luminescence was found to be strongly air-sensitive; the long-lived photoexcited states of **1**$^+$ and **2**$^+$ are efficiently quenched by dioxygen molecules (Fig. 4a and Fig. S11). The quantum yields of the emission of **1**$^+$ and **2**$^+$ in air-saturated dichloromethane are 0.004 and 0.002, respectively, which are one hundredth of those in degassed one. The lifetimes of the emission of **1**$^+$ and **2**$^+$ in air-saturated dichloromethane are 0.3 μs and 0.2 μs, respectively, which are also one hundredth of those in degassed one. The values of k_r of **1**$^+$ and **2**$^+$ in air-saturated dichloromethane are 1.2×10^4 s^{-1} and 0.7×10^4 s^{-1}, respectively, which are not so different from those in degassed one. In contrast, the values of k_{nr} of **1**$^+$ and **2**$^+$ in air-saturated dichloromethane are 3×10^6 s^{-1} and 5×10^6 s^{-1}, respectively, which are as hundredth large as those in the degassed condition. The large increase in the non-radiative decay should be caused by the fast quenching by the dioxygen molecules in the solution.

Red-shift and a decrease in the intensity of the emission upon cooling were observed in dichloromethane solution of **1**$^+$ (Fig. 4b). The λ_{em} of the emission of **1**$^+$ at 298 K, 253 K, and 213 K in CH_2Cl_2 are 570 nm, 585 nm, 595 nm, respectively. The lifetimes of the emission under the same conditions are $\tau =$ 26 μs, 65 μs, and 80 μs, respectively. The temperature dependence is typical for the delayed fluorescence which is characteristic of the emission of the copper(I) complexes.[9-12]

The values of k_r at 253 K and 213 K are much smaller than that at 298 K, because the contribution of the thermally-activated-fluorescence at lower temperature is reduced than that at higher temperature (Table S3). The values of k_{nr} at 253 K and 213 K are also smaller than that at 298 K, but the decrease in k_r at low temperature is more remarkable than that in k_{nr}. Therefore the emission intensities at lower temperature are weaker than those at higher temperature.

DFT calculations for $\mathbf{1}^+$ and $\mathbf{2}^+$ were performed in order to examine the photophysics of the complexes. The results are tabulated in Table 2 and Table 3, and the Kohn-Sham orbitals are displayed in Fig. 5. Details of the results of the calculations are tabulated in Table S4, S5, S6, and S7. The optimized structures in the singlet ground state (S_0) of both $\mathbf{1}^+$ and $\mathbf{2}^+$ were used in the population analysis and TDDFT calculations.

The HOMO, HOMO-1, and HOMO-2 of $\mathbf{1}^+$ mainly consist of the copper (54% for HOMO, 78% for HOMO-1, 76% for HOMO-2) atom orbitals with minor contribution of the phosphorus atoms as well as phenyl groups in diop moiety (Table 2, Table S4, and Table S5). In contrast, LUMO and LUMO+1 of $\mathbf{1}^+$ have major components of the π* orbitals of the phenanthroline moiety. The contributions of Ph_{NN} in LUMO and LUMO+1 are small but not negligible, and those in HOMO-3 and HOMO-4 are significant (31% for HOMO-3 and 62% for HOMO-4). This result suggests that the phenyl groups, Ph_{NN}, which are not parallel to the phenanthroline plane, can significantly affect the photophysics of the complexes. The population for these orbitals of $\mathbf{2}^+$ is basically similar to that of $\mathbf{1}^+$, except for the orbitals related to the phenyl groups on the phenanthroline moiety.

TDDFT calculation for $\mathbf{1}^+$ indicates that the largest component of the transition from ground (S_0) to singlet lowest-lying excited (S_1) states ($S_0 \rightarrow S_1$) is HOMO→LUMO, which can be represented as a CT transition from an orbital consist of copper and phosphorous atomic orbitals to π* orbitals of diimine moiety (Table 3, Table S6 and Table S7). The component of HOMO-1→LUMO also contributes to the CT transition mentioned above. The calculated energy of the wavelength of $\mathbf{1}^+$ is 427 nm, which is close to the experimental value obtained from lowest-energy, suggesting that the absorption is assigned as the CT transition, which is characteristic of a family of $[Cu(NN)(PP)]^+$.[9-11] Other calculated transitions, shown in Table 3, from ground to upper excited states are related to the components of the CT transition, such as HOMO→LUMO+1, or the π-π* transitions of the phenanthroline moiety, such as HOMO-3→LUMO and HOMO-4→LUMO+1.

The character of the transition of $\mathbf{2}^+$ is similar to that of $\mathbf{1}^+$. For example, the $S_0 \rightarrow S_1$ transition has a major component of HOMO→LUMO, which is assigned as the CT transition mentioned above. The calculated energy of the $S_0 \rightarrow S_1$ transition of $\mathbf{2}^+$ (432 nm) is red-shifted from that of $\mathbf{1}^+$ (427 nm), whereas experimental absorption of $\mathbf{2}^+$ (374 nm) in dichloromethane is blue-shifted from that of $\mathbf{1}^+$ (382 nm). The value of f of $\mathbf{1}^+$ is approximately twice as large as that of $\mathbf{2}^+$. The increase of the value of f can be caused by the effects of the introduction of Ph_{NN}. The contribution of the Ph_{NN} moieties to the LUMO, LUMO+1, HOMO-3 and HOMO-4 as described above should be the main reason why almost all oscillator strength values of $\mathbf{1}^+$ are large than that of $\mathbf{2}^+$.

The largest component among the transitions from ground to triplet excited (T_1) states ($S_0 \rightarrow T_1$) of $\mathbf{1}^+$ is HOMO→LUMO+1, which is also represented as the CT transition from an orbital, which consists of copper and phosphorous atomic orbitals, to the π* orbital of phenanthroline moiety. The energy of the $S_0 \rightarrow T_1$ transition of $\mathbf{1}^+$ is 476 nm, which is shorter than the experimental emission spectra (570 nm) in the solution state. The difference between calculated and experimental values is due to the fact that the structural relaxation in the excited state of $[Cu(NN)(PP)]^+$ is generally large. The difference in the calculated energy between $S_0 \rightarrow S_1$ (23400 cm^{-1}) and $S_0 \rightarrow T_1$ (21000 cm^{-1}) transitions is small (2400 cm^{-1}) compared to normal organic compounds. The calculation is consistent with the fact that the observed emission at room temperature is derived from delayed fluorescence which is characteristic of the luminescence of $[Cu(NN)_2]^+$ and a family of $[Cu(NN)(PP)]^+$.[9-11] The experimental results of the temperature dependence of the emission spectra also support the mechanism. The trend in the $S_0 \rightarrow T_1$ transition of $\mathbf{2}^+$ is basically similar to that of $\mathbf{1}^+$. It should be noted that the calculated $S_0 \rightarrow T_1$ transition of $\mathbf{1}^+$ has the contribution of the orbitals HOMO-3, HOMO-4, HOMO-11, HOMO-13, and HOMO-21, which show significant amplitude at the Ph_{NN} groups in the phenanthroline moiety. These contributions should be one of the origins of the remarkable photophysical properties of $\mathbf{1}^+$.

Conclusion

A highly emissive copper(I) complex bearing dmpp and diop, $\mathbf{1}\cdot PF_6$, was newly synthesized, and the photophysics of $\mathbf{1}\cdot PF_6$ and its dmp analogue, $\mathbf{2}\cdot PF_6$, were examined in detail. The diop ligand is very effective to increase the quantum yield and the lifetime of the luminescence. One of the important reasons for the enhancement is the decrease of the apparent non-radiative constant. These emission properties are found to be enhanced by the introduction of Ph_{NN}, the phenyl groups at 4- and 7-positions of phenanthroline. The nature of the luminescence is charge transfer from both copper and phosphorus atom orbitals to π* orbitals of diimine moieties. This finding is important for development of photofunctional materials and utilization of light energy.

Acknowledgements

This work was financially supported by Grants-in-Aid from MEXT of Japan (26410077), the Promotion and Mutual Aid Corporation for Private Schools of Japan, and Grant from Seikei University.

Notes and references

[a] Department of Materials and Life Science, Seikei University, Kichijoji-kitamachi, Musashino, Tokyo 180-8633, Japan. E-mail: tsubomura@st.seikei.ac.jp; Fax: +81-422-37-3871; Tel. +81-422-37-3752.

[b] Research Laboratory for Nuclear Reactors, Tokyo Institute of Technology, 2-12-1 Ōokayama, Meguro-ku, Tokyo 152-8550, Japan.

Electronic Supplementary Information (ESI) available: Crystallographic data for X-ray structural analysis, NMR spectra, emission spectra, and details of the DFT calculations. See DOI: 10.1039/b000000x/

1 B. O'Regan and Grätzel, M. *Nature*, 1991, **353**, 737–740.
2 M. A. Baldo, D. F. O'Brien, Y. You, A. Shoustikov, S. Sibley, M. E. Thompson and S. R. Forrest, *Nature*, 1998, **395**, 151–154.
3 M. A. Baldo, M. E. Thompson and S. R. Forrest, *Nature*, 2000, **403**, 750–753..
4 T. J. Meyer, *Acc. Chem. Res.* 1989, **22**, 163–170.
5 J.-P. Sauvage, *Bull. Jpn. Soc. Coord. Chem.*, 2010, **55**, 3–18.
6 J.-P. Collin, C. Dietrich-Buchecker, P. Gaviña, M. C. Jiménez-Molero and J.-P. Sauvage, *Acc. Chem. Res.*, 2001, **34**, 477–487.

7 M. Nishikawa, K. Nomoto, S. Kume and H. Nishihara, *J. Am. Chem. Soc.*, 2012, **134**, 10543–10553.

8 M. Nishikawa, S. Kume and H. Nishihara, *Phys. Chem. Chem. Phys.*, 2013, **15**, 10549–10565.

9 (a) N. Armaroli, G. Accorsi, F. Cardinali and A. Listorti, *Top. Curr. Chem.*, 2007, **280**, 69–115. (b) A. Barbieri, G. Accorsi and N. Armaroli *Chem. Commun.*, 2008, 2185–2193.

10 A. Lavie-Cambot, M. Cantuel, Y. Leydet, G. Jonusauskas, D. M. Bassani and N. D. McClenaghan, *Coord. Chem. Rev.*, 2008, **252**, 2572–2584.

11 D. R. McMillin and K. M. McNett, *Chem. Rev.*, 1998, **98**, 1201–1219.

12 (a) Siddique, Z. A.; Yamamoto, Y.; Ohno, T.; Nozaki, K. *Inorg. Chem.* **2003**, 42, 6366-6378. (b) Q. Zhang, T. Komino, S. Huang, S. Matsunami, K. Goushi, and C. Adachi, *Adv. Funct. Mater.*, 2012, **22**, 2327–2336. (c) M. S. Asano, K. Tomiduka, K. Sekizawa, K. Yamashita, and K. Sugiura, *Chem. Lett.*, 2010, **39**, 376–378.

13 D. G. Cuttell, S. M. Kuang, P. E. Fanwick, D. R. McMillin, and R. A. Walton, *J. Am. Chem. Soc.*, 2002, **124**, 6–7.

14 S. M. Kuang, D. G. Cuttell, D. R. McMillin, P. E. Fanwick and R. A. Walton, *Inorg. Chem.*, 2002, **41**, 3313–3322.

15 C.-W. Hsu, C.-C. Lin, M.-W. Chung, Y. Chi, G.-H. Lee, P.-T. Chou, C.-H. Chang and P.-Y. Chen, *J. Am. Chem. Soc.*, 2011, **133**, 12085–12099.

16 R. D. Costa, D. Tordera, E. Ortí, H. J. Bolink, J. Schönle, S. Graber, C. E. Housecroft, E. C. Constable and J. A. Zampese, *J. Mater. Chem.*, 2011, **21**, 16108–16118.

17 Andrés-Tomé, I.; Fyson, J.; Dias, F. B.; Monkman, A. P.; Iacobellis, G.; Coppo, P. *Dalton Trans.* 2012, **41**, 8669–8674.

18 C. L. Linfoot, P. Richardson, T. E. Hewat, O. Moudam, M. M. Forde, A. Collins, F. White and N. Robertson, *Dalton Trans.*, 2010, **39**, 8945–8956.

19 Q. Zhang, Q. Zhou, Y. Cheng, L. Wang, D. Ma, X. Jing and F. Wang, *Adv. Mater.*, 2004, **16**, 432–436.

20 S.-P. Luo, E. Mejía, A. Friedrich, A. Pazidis, H. Junge, A.-E. Surkus, R. Jackstell, S. Denurra, S. Gladiali, S. Lochbrunner, and M. Beller, *Angew. Chem. Int. Ed.*, 2013, **52**, 419–423.

21 B. Bozic-Weber, S. Y. Brauchli, E. C. Constable, S. O. Fürer, C. E. Housecroft, F. J. Malzner, I. A. Wright, and J. A. Zampese, *Dalton Trans.*, 2013, **42**, 12293.

22 M. Sandroni, M. Kayanuma, M. Rebarz, H. Akdas-Kilig, Y. Pellegrin, E. Blart, H. Le Bozec, C. Daniel, and F. Odobel, *Dalton Trans.*, 2013, **42**, 14628.

23 C. S. Smith, C. W. Branham, B. J. Marquardt and K. R. Mann, *J. Am. Chem. Soc.*, 2010, **132**, 14079–14085.

24 J. Min, Q. Zhang, W. Sun, Y. Cheng, and L. Wang, *Dalton Trans.*, 2011, **40**, 686.

25 X. Liu, W. Sun, L. Zou, Z. Xie, X. Li, C. Lu, L. Wang, and Y. Cheng, *Dalton Trans.*, 2012, **41**, 1312.

26 X. Liu, H. Nan, W. Sun, Q. Zhang, M. Zhan, L. Zou, Z. Xie, X. Li, C. Lu, and Y. Cheng, *Dalton Trans.*, 2012, **41**, 10199.

27 M. G. Crestani, G. F. Manbeck, W. W. Brennessel, T. M. McCormick, and R. Eisenberg, *Inorg. Chem.*, 2011, **50**, 7172–7188.

28 N. Armaroli, G. Accorsi, M. Holler, O. Moudam, J.-F. Nierengarten, Z. Zhou, R. T. Wegh and R. Welter, *Adv. Mater.*, 2006, **18**, 1313–1316.

29 K. Saito, T. Arai, N. Takahashi, T. Tsukuda, T. Tsubomura, *Dalton Trans.*, 2006, 4444–4448.

30 (a) T. Tsukuda, A. Nakamura, T. Arai and T. Tsubomura, *Bull. Chem. Soc. Jpn.*, 2006, **79**, 288–290. (b) T. Tsubomura, T. Tsukuda and K. Matsumoto, *Bull. Jpn. Soc. Coord. Chem.* 2008, **52**, 29–42. (c) M. Nishikawa and T. Tsubomura, *Bull. Chem. Soc. Jpn.*, DOI:10.1246/bcsj.20140069.

31 S. Sakaki, H. Mizutani, Y. Kase, K. Inokuchi, T. Arai and T. Hamada, *J. Chem. Soc., Dalton Trans.,* 1996, 1909.

32 (a) J. R. Kirchhoff, R. E. Gamache, M. W. Blaskie, A. A. Del Paggio, R. K. Lengel and D. R. McMillin, *Inorg. Chem.*, 1983, **22**, 2380–2384. (b) M. Ruthkosky, F. N. Castellano and G. J. Meyer, *Inorg. Chem.*, 1996, **35**, 6406–6412.

33 H. Doucet, T. Ohkuma, K. Murata, T. Yokozawa, M. Kozawa, E. Katayama, A. F. England, T. Ikariya and R. Noyori, *Angew. Chem., Int. Ed.*, 1998, **37**, 1703–1707.

34 J.-X. Li, Z.-X. Du, H.-Q. An, J. Zhou, J.-X. Dong, S.-R. Wang, B.-L. Zhu, S.-M. Zhang, S.-H. Wu and W.-P. Huang, *J. Mol. Struct.* 2009, 935, 161-166.

35 Luminescence and photo-induced electron transfer properties of **2**·ClO_4 have been reported, but most of the data described in this manuscript have not been mentioned in the Sakaki's paper. S. Sakaki, T. Satoh and K. Ohkubo, *New. J. Chem.*, 1986, **10**, 145–147.

36 P. Coppens, I. I. Vorontsov, T. Graber, A. Y. Kovalevsky, F. Chen, G. Wu, M. Gembicky and I. V. Novozhilova, *J. Am. Chem. Soc.*, 2004, **126**, 5980.

37 (a) G. J. Kubas, *Inorg. Synth.*, 1979, **19**, 90–92. (b) J. R. Kirchhoff, R. E. Gamache, M. W. Blaskie, A. A. Del Paggio, R. K. Lengel and D. R. McMillin, *Inorg. Chem.*, 1983, **22**, 2380–2384.

38 G. R. Fulmer, A. J. M. Miller, N. H. Sherden, H. E. Gottlieb, A. Nudelman, B. M. Stoltz, J. E. Bercaw, and K. I. Goldberg, *Organometallics*, 2010, **29**, 2176–2179.

39 K. Suzuki, A. Kobayashi, S. Kaneko, K. Takehira, T. Yoshihara, H. Ishida, Y. Shiina, S. Oishi, and S. Tobita, *Phys. Chem. Chem. Phys.*, 2009, **11**, 9850.

40 Rigaku (2000). *CrystalClear.* Rigaku Corporation, Tokyo, Japan.

41 A. Altomare, G. Cascarano, C. Giacovazzo, A. Guagliardi, M. C. Burla, G. Polidori and M. Camalli, *J. Appl. Crystallogr.*, 1994, **27**, 435–436.

42 G. M. Sheldrick, *Acta Crystallogr., Sect. A: Fundam. Crystallogr.*, 2007, **64**, 112–122.

43 Farrugia, L. J. *J. Appl. Cryst.* 1999, 32, 837–838.

44 M. J. Frisch, G. W. Trucks, H. B. Schlegel, G. E. Scuseria, M. A. Robb, J. R. Cheeseman, J. A. Montgomery, Jr., T. Vreven, K. N. Kudin, J. C. Burant, J. M. Millam, S. S. Iyengar, J. Tomasi, V. Barone, B. Mennucci, M. Cossi, G. Scalmani, N. Rega, G. A. Petersson, H. Nakatsuji, M. Hada, M. Ehara, K. Toyota, R. Fukuda, J. Hasegawa, M. Ishida, T. Nakajima, Y. Honda, O. Kitao, H. Nakai, M. Klene, X. Li, J. E. Knox, H. P. Hratchian, J. B. Cross, V. Bakken, C. Adamo, J. Jaramillo, R. Gomperts, R. E. Stratmann, O. Yazyev, A. J. Austin, R. Cammi, C. Pomelli, J. W. Ochterski, P. Y. Ayala, K. Morokuma, G. A. Voth, P. Salvador, J. J. Dannenberg, V. G. Zakrzewski, S. Dapprich, A. D. Daniels, M. C. Strain, O. Farkas, D. K. Malick, A. D. Rabuck, K. Raghavachari, J. B. Foresman, J. V. Ortiz, Q. Cui, A. G. Baboul, S. Clifford, J. Cioslowski, B. B. Stefanov, G. Liu, A. Liashenko, P. Piskorz, I. Komaromi, R. L.

Martin, D. J. Fox, T. Keith, M. A. Al-Laham, C. Y. Peng, A. Nanayakkara, M. Challacombe, P. M. W. Gill, B. Johnson, W. Chen, M. W. Wong, C. Gonzalez, and J. A. Pople, Gaussian, Inc., Wallingford CT, 2004.

45 A. D. J. Beck, *Chem. Phys.*, 1992, **96**, 2155‑2160.

46 A. D. J. Becke, *Chem. Phys.*, 1993, **98**, 5648‑5652.

47 C. Lee, W. Yang and R. G. Parr, *Phys. Rev.*, 1988, **B37**, 785.

48 A. J. H. Wachters, *J. Chem. Phys.*, 1970, **52**, 1033‑1036.

49 S. I. Gorelsky, *AOMix*: Program for Molecular Orbital Analysis, University of Ottawa, 2011.

50 U. Varetto, *Molekel*, Swiss National Supercomputing Centre: Lugano, Switzerland.

51 Apparent radiative and non-radiative constants are defined as $k_r = \Phi / \tau$ and $k_{nr} = (1-\Phi) / \tau$, respectively.

52 The quantum yield for $[Cu(dmp)(DPEphos)]^+$ was reported to 0.15 based on the standard value ($\Phi = 0.042$ for $[Ru(bpy)_3]^{2+}$ in deoxygenated water).[14] If the recently reported value of 0.06 (Reference 39) is employed for the standard, the value for $[Cu(dmp)(DPEphos)]^+$ should be 0.23. In this case, k_r and k_{nr} of $[Cu(dmp)(DPEphos)]^+$ are calculated to be 1.6×10^4 s^{-1} and 5.4×10^4 s^{-1}, respectively. Even if these values are correct, the k_{nr} of **2**$^+$ is significantly lower than that of the DPEphos complex.

Highly Emissive Copper(I) Complexes Bearing Diimine and Bis(diphenylphosphinomethyl)-2,2-dimethyl-1,3-dioxolane

Michihiro Nishikawa, Shota Sawamura, Aya Haraguchi, Jun Morikubo, Koichiro Takao and Taro Tsubomura*

TOC graphic

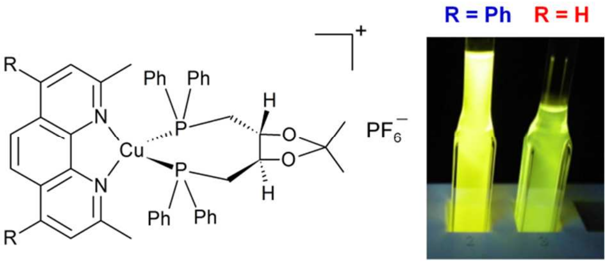

Highly emissive copper(I) complexes bearing 4,5-bis(diphenylphosphinomethyl)-2,2-dimethyl-1,3-dioxolane and 1,10-phenanthroline derivative were newly synthesized. The quantum yields of the photoluminescence are up to 0.38.